Report

Current Biology

Locomotion and Task Demands Differentially Modulate Thalamic Audiovisual Processing during Active Search

Highlights

- Auditory thalamic activity is significantly suppressed during movement
- Visual thalamic activity is subtly enhanced, only at high running speeds
- Behavioral relevance modulates activity in visual—but not auditory—thalamus
- Locomotor state and task relevance can be used to improve neural decoding accuracy

Authors

Ross S. Williamson, Kenneth E. Hancock, Barbara G. Shinn-Cunningham, Daniel B. Polley

Correspondence

ross_williamson@meei.harvard.edu

In Brief

Williamson et al. recorded from the auditory and visual thalamus of mice engaged in an audiovisual search task. They find a double dissociation between task relevance and movement, highlighting a role for modulation of thalamic responses by internal state and suggesting key differences in modulatory circuitry between auditory and visual pathways.

Williamson et al., 2015, Current Biology *25*, 1–7
July 20, 2015
http://dx.doi.org/10.1016/j.cub.2015.05.045

CellPress

Please cite this article in press as: Williamson et al., Locomotion and Task Demands Differentially Modulate Thalamic Audiovisual Processing during Active Search, Current Biology (2015), http://dx.doi.org/10.1016/j.cub.2015.05.045

Current Biology
Report

Locomotion and Task Demands Differentially Modulate Thalamic Audiovisual Processing during Active Search

Ross S. Williamson,[1,2,*] Kenneth E. Hancock,[1,3] Barbara G. Shinn-Cunningham,[2] and Daniel B. Polley[1,2,3]
[1]Massachusetts Eye and Ear Infirmary, Eaton-Peabody Laboratories, 243 Charles Street, Boston, MA 02114, USA
[2]Center for Computational Neuroscience and Neural Technology, Boston University, 677 Beacon Street, Boston, MA 02215, USA
[3]Department of Otology and Laryngology, Harvard Medical School, 25 Shattuck Street, Boston, MA 02115, USA
*Correspondence: ross_williamson@meei.harvard.edu
http://dx.doi.org/10.1016/j.cub.2015.05.045

SUMMARY

Active search is a ubiquitous goal-driven behavior wherein organisms purposefully investigate the sensory environment to locate a target object. During active search, brain circuits analyze a stream of sensory information from the external environment, adjusting for internal signals related to self-generated movement or "top-down" weighting of anticipated target and distractor properties. Sensory responses in the cortex can be modulated by internal state [1–9], though the extent and form of modulation arising in the cortex de novo versus an inheritance from subcortical stations is not clear [4, 8–12]. We addressed this question by simultaneously recording from auditory and visual regions of the thalamus (MG and LG, respectively) while mice used dynamic auditory or visual feedback to search for a hidden target within an annular track. Locomotion was associated with strongly suppressed responses and reduced decoding accuracy in MG but a subtle increase in LG spiking. Because stimuli in one modality provided critical information about target location while the other served as a distractor, we could also estimate the importance of task relevance in both thalamic subdivisions. In contrast to the effects of locomotion, we found that LG responses were reduced overall yet decoded stimuli more accurately when vision was behaviorally relevant, whereas task relevance had little effect on MG responses. This double dissociation between the influences of task relevance and movement in MG and LG highlights a role for extrasensory modulation in the thalamus but also suggests key differences in the organization of modulatory circuitry between the auditory and visual pathways.

RESULTS

Mice Can Use Dynamic Audiovisual Feedback to Search for Hidden Rewards

We adapted a closed-loop sensory foraging task [13–15] to explore how behavioral state modulates thalamic sensory processing. The task required mice to locate a hidden target region within an annular track to obtain a water reward. Every 0.5 s, mice were presented with pairs of visual flashes or acoustic chirps. The temporal interval separating individual flashes or chirps within the pair switched from long to short as mice moved into the visual or auditory target regions, respectively (Figure 1A). Water reward was contingent upon remaining within the target region for one modality, but not the other, with the choice of modality assigned randomly to each mouse. This arrangement ensured that a change in the inter-pulse interval was task relevant (TR) for one modality but was a task-irrelevant (TI) distraction for the other. After a period of behavioral shaping (see Supplemental Experimental Procedures), a 32-channel silicon probe was implanted into the thalamus at an orientation that enabled simultaneous recordings from the medial geniculate body and dorsal lateral geniculate nucleus of the thalamus (MG and LG, respectively; Figure 1B). This approach allowed us to record from each thalamic subdivision during periods of movement or rest and to contrast responses in mice where vision was TR and audition was TI (Figure 1C) versus mice trained with the opposite stimulus-reward contingency (Figure 1D).

This type of closed-loop active search behavior eschews the rigid structure of conventional psychophysical tasks in favor of an ethologically relevant foraging behavior wherein mice are free to modulate their search speed and movement trajectories according to real-time changes in sensory feedback [16, 17]. On some trials, mice quickly doubled back into the TR target region after crossing through it (Figure 2A), whereas on others, mice circled clockwise and counter-clockwise around the entire track several times before settling on the TR target region (Figure 2B). To test whether search behavior was under stimulus control, we measured the probability that mice would remain within a target region long enough to trip the reward for the TR modality versus pause within the TI target region for an equivalent length of time (TR: visual [n = 3]; TR: auditory [n = 3]). When initially introduced to the behavioral task, mice were as likely to pause within the TR target region as they were the TI target or a randomly selected region (Figure 2C, left; ANOVA; main effect for task relevance; $F_{2,2} < 0.7$; $p > 0.5$ for both groups). With additional weeks of training, mice exhibited a significant choice bias, such that the probability of pausing within the TR target region was significantly greater than the probability of selecting either the target for the TI modality or a randomly selected region (Figure 2C, right; ANOVA; main effect for task relevance; $F_{2,2} > 15.0$; $p < 0.02$ for both groups). As further evidence that

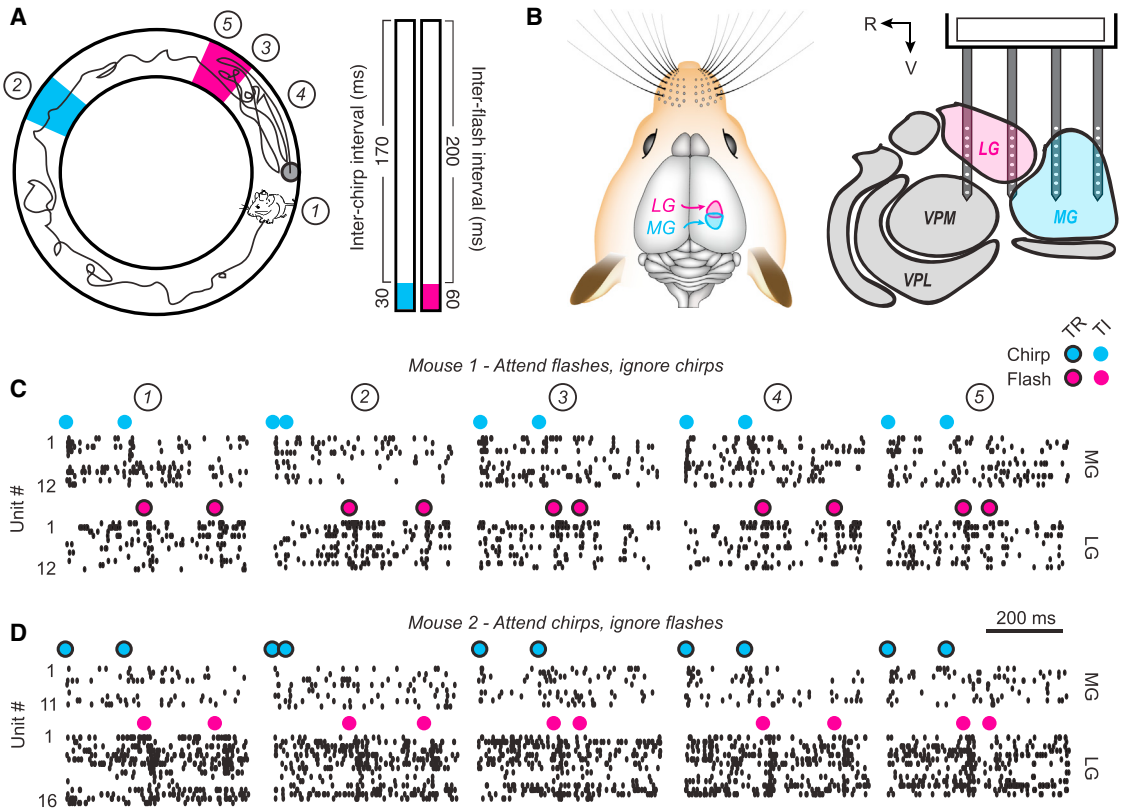

Figure 1. Recording from Auditory and Visual Subdivisions of the Mouse Thalamus during an Active Search Task

(A) Illustration of a mouse's movement path (thin black line) within the annular track during a single behavioral trial. Cyan and magenta areas correspond to short-interval target regions for auditory and visual pulse pairs, respectively. Gray circle represents the water reward spout. Circled numbers correspond to unit recordings below.

(B) The medial geniculate body (cyan; MG) and dorsal lateral geniculate nucleus (magenta; LG) schematized from a dorsal (left) and sagittal (right) perspective. The positioning of the 32-channel probe is shown on the right. R, rostral; V, ventral.

(C and D) Rastergrams compiled from ensembles of 11–16 simultaneously recorded MG (top rows) and LG (bottom rows) units from one mouse trained to associate changes in the visual inter-flash interval with reward (C) and another mouse trained to associate changes in the auditory inter-chirp interval with reward (D). TR and TI denote whether the corresponding modality provides the sole cue to identify the hidden target (TR) or is a distractor (TI). Rastergrams are drawn from five 0.5-s epochs recorded at positions approximately corresponding to the numbered locations in (A).

behavior was under stimulus control, we observed that checking the water spout for reward availability was far more likely after pausing within the TR target region than after pausing within the TI target or a random position in well-trained mice (Figure 2D, right; ANOVA; main effect for task relevance; $F_{2,2} > 20.0$; $p < 0.01$ for both groups).

A Double Dissociation in Thalamic Response Modulation by Internal State

The set of behaviors that naturally occur during this task provided us with a means to estimate the influence of internal modulatory signals such as either locomotion or task demands on LG and MG unit activity. Running increases the gain on visually evoked responses in the visual cortex [5, 18–20] but attenuates sound-evoked responses in the auditory cortex [8, 9, 12]. Subcortical antecedents for movement-related response modulation are less clear. Initial characterization of locomotion effects reported no change in sensory-evoked LG or MG responses during periods of movement versus rest [5, 8], though subsequent studies suggest that a comparatively subtle degree of gain and attenuation may be occurring in the LG and MG, respectively [9, 12, 21].

To clarify the effect of locomotion on thalamic responses, we contrasted LG and MG spike rates during periods of movement and rest. We found that sound-evoked firing rates in MG were reduced in 94.1% of all recorded units (n = 474) by an average of 15.1% during movement, whereas spontaneous activity was not affected (bootstrapped ANOVA; main effect for locomotion: evoked, $F_{1,46} = 52.36$, $p < 1 \times 10^{-20}$; spontaneous, $F_{1,46} = 8.15$, $p = 0.17$; Figure 3A). Significant movement-related suppression was noted in recordings from both putative dorsal and ventral subdivisions of the MG (Figures S1A and S1B). By contrast, locomotion was not associated with significant changes in either visually evoked or spontaneous firing rates in the LG (mean change = 2.1% increase; n = 518 units; bootstrapped ANOVA; main effect for locomotion: evoked, $F_{1,73} = 3.17$, $p = 0.7$; spontaneous, $F_{1,73} = 2.23$, $p = 0.82$; Figure 3A). Similar movement-related changes in LG and MG firing rates were noted on trials when mice were disengaged from the behavioral task, suggesting that the locomotion effects described here

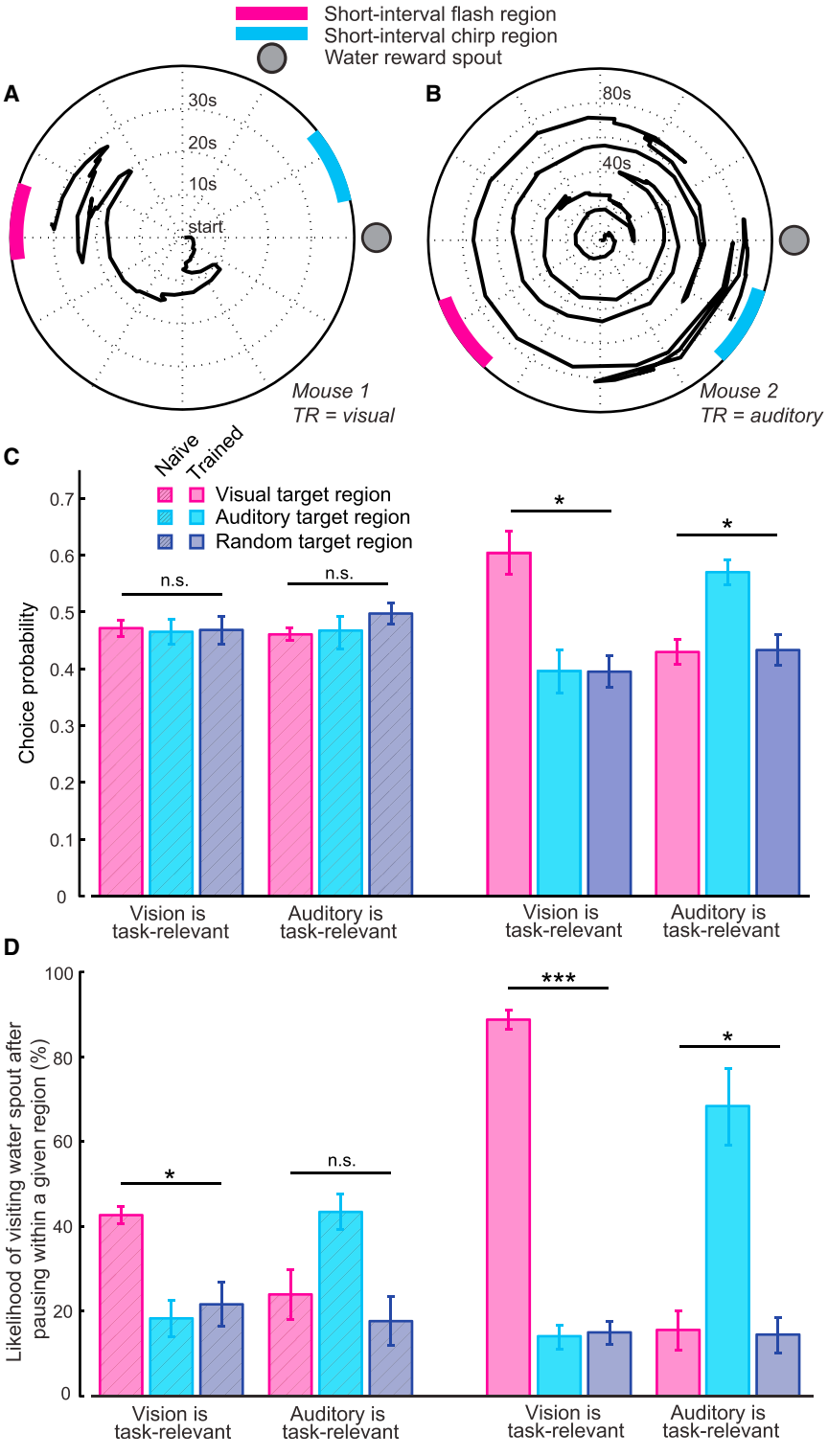

Figure 2. Mice Learn to Recognize Changes in Temporal Interval within the Task-Relevant Stimulus Modality

(A and B) Polar plots illustrate the mouse's position on the annular track as a function of time (radial axis, in seconds) relative to visual (magenta) and auditory (cyan) target locations. Each plot depicts a single, representative trial from a mouse where vision was the TR modality (A) and another mouse where auditory was the TR modality (B).

(C) The operational definition of behavioral choice is satisfied when the mouse remained within a single target region for at least 1.5–1.75 s. The probability that mice would initially choose the target region linked to reward or the TI target region is plotted for visual-TR (n = 3) and for auditory-TR mice (n = 3). Bias for pausing within the TR target region is evident in trained mice, but not in naive mice (hatched).

(D) Mice develop a selective bias for returning to the water spout after pausing within the TR target region. Behavioral data for the naive condition are drawn from the first 20% of trials (C) or the first 100 trials (D). Values reflect mean ± SEM. Asterisks denote statistically significant differences ($p < 0.05$) with a two-way ANOVA.

are consistent with previous descriptions of movement-related modulation reported in head-fixed mice that are not engaged in an explicit task (Figures S1C and S1D) [5, 9, 12, 18–21].

Moving and stationary are but two discrete states along a locomotion continuum. By quantifying the change in firing rate across the full range of observed movement speeds, we noted a monotonic increase in sound-evoked suppression with running speed in MG. Surprisingly, LG firing rates were modestly but significantly increased at high running speeds (ANOVA; main effect for running speed: MG, $F_{16,473} = 29.01$, $p = 5.32 \times 10^{-86}$; LG, $F_{16,517} = 3.36$, $p = 6.11 \times 10^{-6}$; Figure 3B). Movement velocities associated with substantive LG firing rate enhancements were uncommon (running speeds that cause >5% suppression occurred in only 17% of all observations; Figure 3C). Thus, as a first approximation, our findings confirm that movement was not associated with changes in LG firing rate [5], though modest increases were noted at uncommonly high running speeds, in keeping with subsequent findings [21]. By contrast, sound-evoked spiking in the MG is suppressed across the full spectrum of locomotion, reaching levels as high as 30% at the highest running speeds. An analysis of movement-related modulation on single-unit firing rates in LG and MG yielded a nearly identical pattern of results to multi-unit recordings (Figure S1D).

In the present study, all mice operated on the same bottom-up statistics of chirp and flash pairs, but they learned that the temporal interval of one modality provided the sole cue about reward availability whereas the other was an uninformative distraction. Thus, simultaneous LG and MG recordings could be made from mice that regarded vision as the TR modality and audition

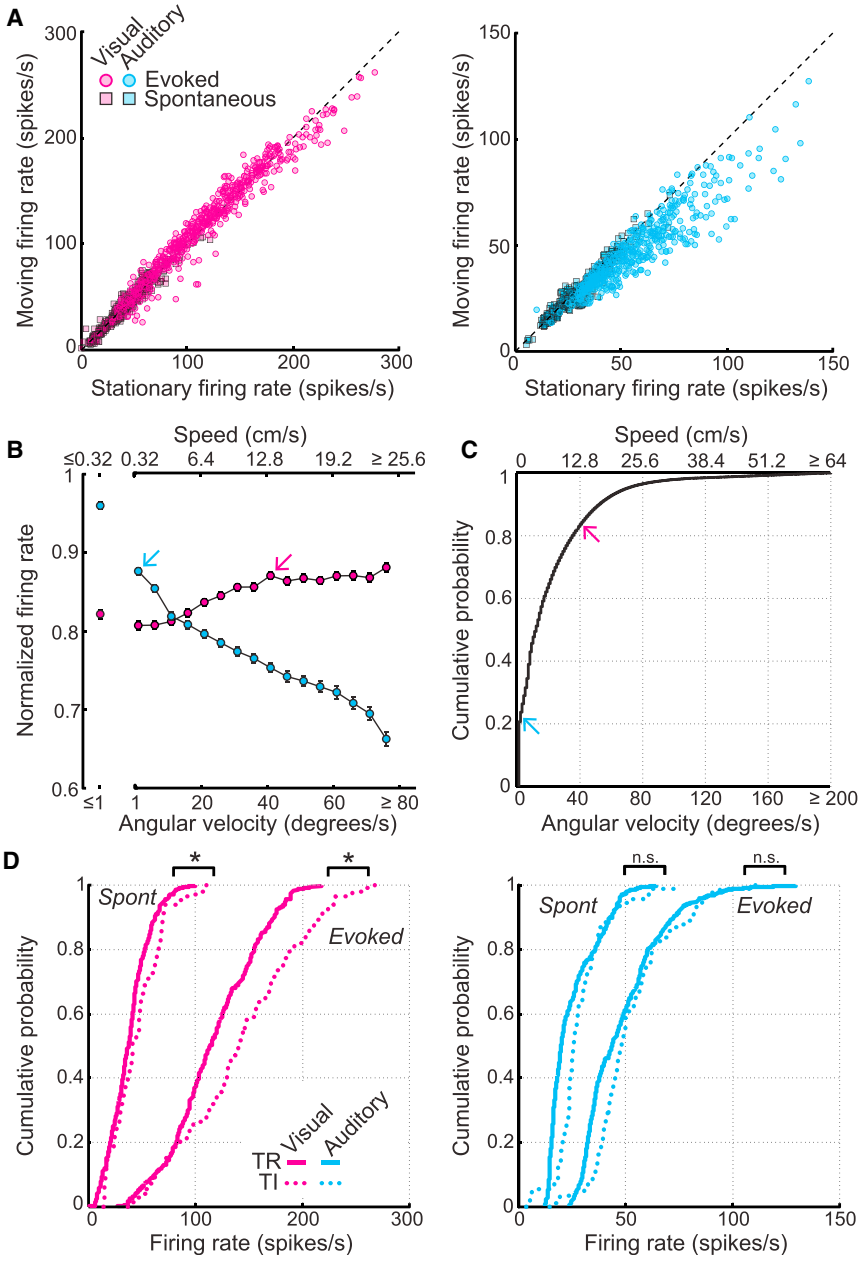

Figure 3. Movement Is Associated with Robust Firing Rate Modulation in MG, but Not LG; Task Relevance Modulates Firing Rates in LG, but Not MG

(A) Scatterplots present the firing rate for all recorded units in LG (left column) and MG (right column). Firing rates were obtained from stimulus-evoked (circles) or spontaneous (squares) PSTH epochs. Each data point is the mean response to both pulses in a given pair for a single recording site averaged across a single behavioral session.

(B) Evoked firing rate as a function of running speed in LG (magenta) and MG (cyan). Firing rates were normalized to the maximum firing rate for each unit. Values reflect mean ± SEM.

(C) Cumulative fraction of times the animals spent at each particular speed. Arrows depict the lowest running speed associated with firing rate modulation ≥5% (B) and the probability that the corresponding running speed occurs (C).

(D) Cumulative firing rate distributions are organized according to task relevance rather than locomotion status for sensory-evoked and spontaneous responses. Asterisks denote statistically significant differences ($p < 0.05$) with a bootstrapped ANOVA.

as the TI modality and another set of mice with reversed TR and TI contingencies. Even though LG units were relatively unaffected by locomotion, changes in LG activity have been reported in the context of other internal state variables such as spatial attention [10, 11, 22]. By contrast, MG firing has been described as comparatively refractory to modulation by "top-down" cognitive signals relating to task demands [4, 23]. Thus, our a priori hypothesis was that firing rates would be increased in the LG—but not MG—when the corresponding modality was TR.

Consistent with this hypothesis, we found that MG firing rates were not significantly changed by the behavioral utility of sound (firing rates were increased by a mean 4.3% in TR versus TI units; bootstrapped ANOVA; $F_{1,46} < 1.65$; $p \geq 0.1$ for evoked and spontaneous contrasts between TR [n = 382] and TI [n = 92] conditions; Figure 3D, right). However, LG firing rates were suppressed by an average of 17.5% when vision was TR compared to TI, with significant reductions evident in both evoked and spontaneous firing rates (TR, n = 367 units; TI, n = 151 units; evoked, $F_{1,73} = 16.14$, $p = 0.01$; spontaneous, $F_{1,73} = 12.51$, $p = 0.04$; Figure 3D, left). Thus, as predicted, LG responses were modulated by behavioral relevance whereas MG responses were not. However, the direction of modulation was unexpected in that LG activity was suppressed when vision was TR, not enhanced.

Ensemble Decoding of Stimulus Identity Recapitulates Firing Rate Modulation

These findings highlight a striking double dissociation in modulation of thalamic response by internal states. Locomotion suppressed sound-evoked responses in the MG but weakly enhanced responses in LG; behavioral relevance was associated with reduced responsiveness in LG but had no significant effect on MG responses. These observations lead us to question how changes in overall unit activity levels related to the goal of the behavioral task, namely, to actively search the annular arena for the hidden TR target region. To address this question, we used a neural classifier to decode whether the mouse was in a target (short interval) or non-target (long interval) region of the behavioral arena based on a single 500 ms "glimpse" of ensemble spiking activity from the LG or MG (Figure 4A).

As a first step, we determined the optimal PSTH bin size for decoding visual and auditory pulse timing. With very small bin

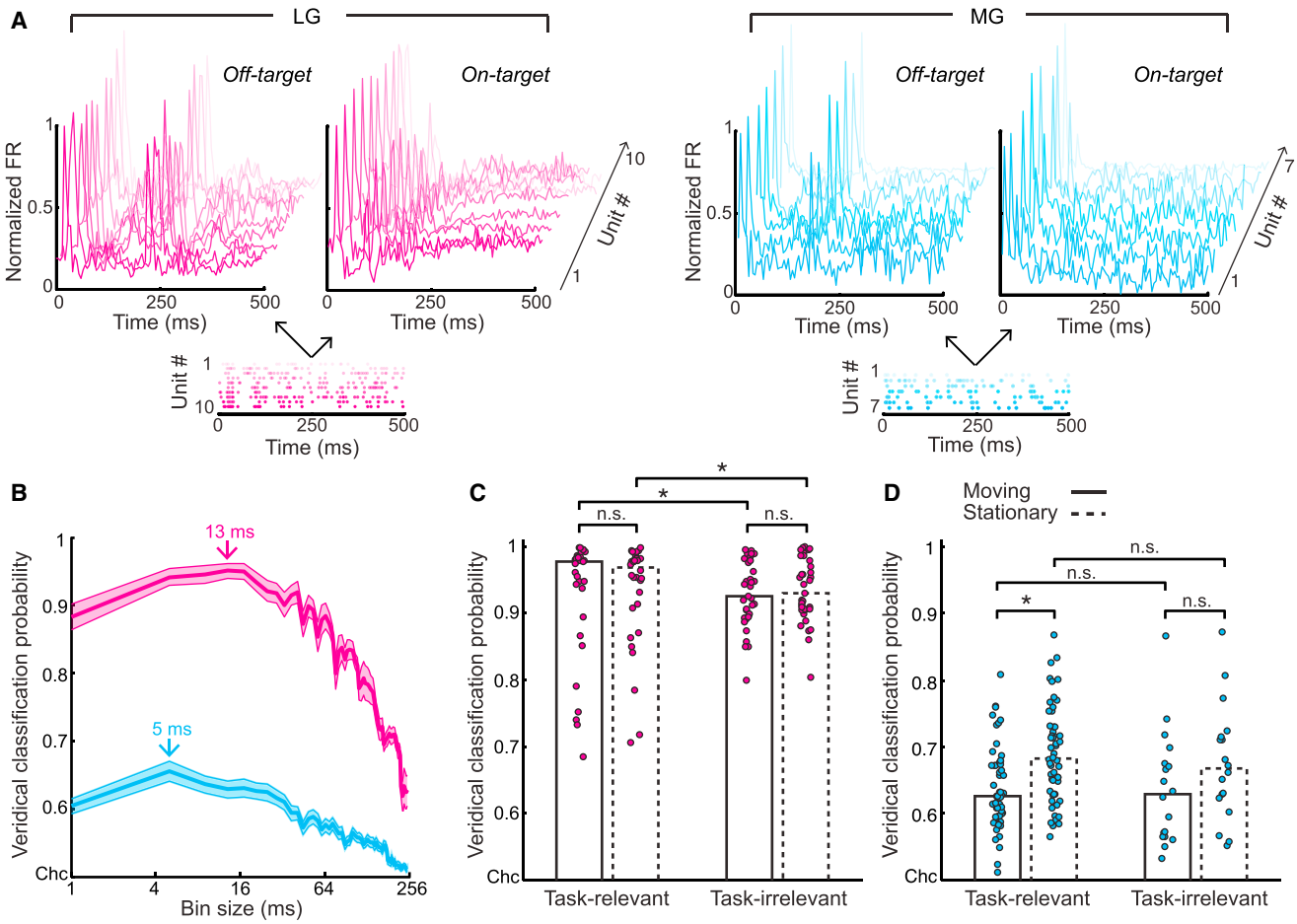

Figure 4. Modulation of Firing Rate by Locomotion and Task Relevance Underlies Differences in Stimulus Decoding Accuracy

(A) Classification of inter-pulse interval based on thalamic ensemble activity recorded during a single behavioral "moment." Shown here are examples of simultaneously recorded LG (n = 10) and MG (n = 7) unit ensembles from a mouse in the visual TR condition. PSTH templates for each unit are averaged from a subset of moments where the mouse was in a long interval non-target area (left) or was inside the short interval target (right). The inter-pulse interval of a given chirp or flash pair was decoded by calculating the shorter Euclidean distance separating a single behavioral moment (rastergrams, bottom) from the target and non-target averaged templates. Euclidean distance between a single trial and each template in the mathematical model is proportional to the length of each corresponding arrow. PSTH templates were averaged from the same number of moments for all four conditions (off-target versus on-target and moving versus stationary) in each brain region (MG and LG) for each mouse, using subsampling (see Supplemental Experimental Procedures). Half of all moments were used to create the corresponding templates, and the other half were used individually for single-moment classification.

(B) Median classification accuracy across all conditions and behavioral sessions as a function of PSTH bin size. Arrows indicate the optimal bin size for MG (cyan) and LG (magenta). Shaded regions = 95% confidence interval; solid lines, median; chance (Chc) classification = 50% accuracy.

(C and D) Inter-pulse interval classification accuracy as a function of task relevance and locomotion for LG (C) and MG (D) ensembles. Each data point represents the mean decoding accuracy from a single behavioral session. Bar height represents the sample median. Asterisks denote statistically significant differences based on permutation tests corrected for multiple comparisons.

sizes (e.g., 1 ms) the internal jitter of spike times degraded the representation of each pulse within the pair. Similarly, larger bin sizes degraded signal-to-noise ratios by incorporating an increasing proportion of spikes that do not directly relate to pulse timing (Figure 4B). Our analysis suggested that pulse rate could be optimally decoded by temporally integrating spikes over a 13-ms window in LG and a 5-ms window in MG, which agrees closely with behavioral inter-pulse interval discrimination threshold values following direct activation of the central visual or auditory cortex, respectively [24].

We then used these optimized bin sizes to contrast differences in inter-pulse interval decoding accuracy within a daily behavioral session as a function of locomotion state and stimulus task relevance. For the most part, differences in decoding accuracy recapitulated the double dissociation in firing rates, although the sign of firing rate change (increase or decrease) was not directly linked to classification accuracy. In the LG, movement had no effect on classification accuracy (permutation test: TR versus TI [n = 32 and 35 behavioral sessions, respectively]; $p > 0.8$ for moving versus stationary for TR and TI conditions; Figure 4C). Although LG firing rates were reduced when vision was TR, the spiking patterns supported a more-accurate classification of visual flash interval (permutation test; $p = 0.01$ for TR versus TI for both moving and stationary

conditions; Figure 4C). Conversely, classification accuracy in MG was not affected by task relevance (permutation test; $p > 0.5$ for both TR versus TI [n = 54 and 18 behavioral sessions, respectively] in moving and stationary conditions; Figure 4D), but the reduced firing rates during movement were associated with lower accuracy in decoding the chirp interval. This difference reached statistical significance in the TR condition, but not in the TI condition (permutation test; $p = 0.0001$ and $p = 0.15$, respectively).

DISCUSSION

We recorded from auditory and visual subdivisions of the thalamus as mice used closed-loop audiovisual feedback to navigate around an annular track in search of a hidden target. The design of the task enabled us to measure whether thalamic sensory responses were modulated by non-sensory signals related to internal state. Previous studies in head-fixed mice placed atop a movable platform demonstrated that locomotion augments visually evoked responses in the visual cortex [5, 20, 25] but attenuates sound-evoked activity in auditory cortex [8, 9, 12]. Evidence on the subcortical origins of these effects are mixed with some studies reporting no evidence of locomotion effects in LG or MG [5, 8] and more-recent reports suggesting that locomotion can impart a comparatively subtle augmentation or suppression in the visual and auditory thalamus, respectively [9, 12, 21]. Our data feature simultaneous recordings from both LG and MG and are unequivocal on this point: movement is associated with a subtle increase in LG responses only at uncommonly high running speeds and has no effect on temporal interval decoding, whereas sound-evoked MG responses are strongly suppressed and decode stimulus identity less accurately across a broad range of running speeds. Importantly, movement-related modulation of thalamic activity in either subdivision is less robust than what has been reported in primary sensory cortex, underscoring the likely involvement of additional intracortical circuits that mediate more-extensive response modulation in downstream processing [8, 9, 12, 20, 21].

At the level of the cortex, sensory traces have been largely reformatted into an abstraction of the source signal [26]. This spatiotemporal pattern of spikes continues to encode relevant features of the stimulus but is also powerfully modulated by non-sensory factors such as emotion, learning, attention, and motor planning [3, 6, 7, 27–31]. Whereas the neural circuitry for extrasensory modulation is exquisite and comparatively well understood in sensory neocortex [9, 12, 20, 25, 32–36], additional modulatory networks in the thalamus [37] or midbrain [38] could provide a means for rapid and flexible adjustments of subcortical auditory [23, 39–41] and visual [10, 42, 43] processing depending on task demands, attentional load, and learning. Here, for example, we report reduced visually evoked responses in LG that nevertheless more accurately encode inter-flash interval when visual inputs are relevant to solving the behavioral task compared to when they are a distraction. The extent to which internal state modulation of subcortical responses is mediated through subcortical modulatory networks versus descending corticofugal modulation remains a promising area for further investigation.

EXPERIMENTAL PROCEDURES

Audiovisual Search Task

All procedures were approved by the Animal Care and Use Committee at Massachusetts Eye and Ear Infirmary and followed the guidelines established by the NIH for the care and use of laboratory animals. Six male C57/BL6 mice, aged 6–8 weeks, were maintained above 80% of their pre-training body weight. During training, mice received their daily water allowance through the behavioral task with additional supplements as needed.

Detailed information on the behavioral task, chronic thalamic recordings, and data analysis can be found in the Supplemental Experimental Methods.

SUPPLEMENTAL INFORMATION

Supplemental Information includes Supplemental Experimental Procedures, one figure, and one table and can be found with this article online at http://dx.doi.org/10.1016/j.cub.2015.05.045.

AUTHOR CONTRIBUTIONS

All authors contributed to experimental design and manuscript editing. R.S.W. collected and analyzed all data. D.B.P. and R.S.W. wrote the manuscript. K.E.H., R.S.W., and D.B.P. developed hardware and software control for the behavioral neurophysiology experiment.

ACKNOWLEDGMENTS

We thank Jason Osborne (HHMI Janelia Farm) for sharing the microdrive design and Jonathon Whitton for guidance with behavioral training. This work was supported by NSF grant DMS-1042134 (R.S.W.) and NIH grants R21DC012894 (to D.B.P.), P30DC05209, and R01DC009477 (to B.G.S.-C.).

Received: January 31, 2015
Revised: April 23, 2015
Accepted: May 22, 2015
Published: June 25, 2015

REFERENCES

1. Fanselow, E.E., and Nicolelis, M.A. (1999). Behavioral modulation of tactile responses in the rat somatosensory system. J. Neurosci. *19*, 7603–7616.
2. Eliades, S.J., and Wang, X. (2003). Sensory-motor interaction in the primate auditory cortex during self-initiated vocalizations. J. Neurophysiol. *89*, 2194–2207.
3. Polley, D.B., Steinberg, E.E., and Merzenich, M.M. (2006). Perceptual learning directs auditory cortical map reorganization through top-down influences. J. Neurosci. *26*, 4970–4982.
4. Otazu, G.H., Tai, L.-H., Yang, Y., and Zador, A.M. (2009). Engaging in an auditory task suppresses responses in auditory cortex. Nat. Neurosci. *12*, 646–654.
5. Niell, C.M., and Stryker, M.P. (2010). Modulation of visual responses by behavioral state in mouse visual cortex. Neuron *65*, 472–479.
6. Niwa, M., Johnson, J.S., O'Connor, K.N., and Sutter, M.L. (2012). Active engagement improves primary auditory cortical neurons' ability to discriminate temporal modulation. J. Neurosci. *32*, 9323–9334.
7. Atiani, S., David, S.V., Elgueda, D., Locastro, M., Radtke-Schuller, S., Shamma, S.A., and Fritz, J.B. (2014). Emergent selectivity for task-relevant stimuli in higher-order auditory cortex. Neuron *82*, 486–499.
8. Zhou, M., Liang, F., Xiong, X.R., Li, L., Li, H., Xiao, Z., Tao, H.W., and Zhang, L.I. (2014). Scaling down of balanced excitation and inhibition by active behavioral states in auditory cortex. Nat. Neurosci. *17*, 841–850.
9. Schneider, D.M., Nelson, A., and Mooney, R. (2014). A synaptic and circuit basis for corollary discharge in the auditory cortex. Nature *513*, 189–194.

10. O'Connor, D.H., Fukui, M.M., Pinsk, M.A., and Kastner, S. (2002). Attention modulates responses in the human lateral geniculate nucleus. Nat. Neurosci. *5*, 1203–1209.
11. McAlonan, K., Cavanaugh, J., and Wurtz, R.H. (2008). Guarding the gateway to cortex with attention in visual thalamus. Nature *456*, 391–394.
12. McGinley, M.J., David, S.V., and McCormick, D.A. (2015). Cortical membrane potential signature of optimal states for sensory signal detection. Neuron *87*, in press. Published online June 11, 2015.
13. Polley, D.B., Heiser, M.A., Blake, D.T., Schreiner, C.E., and Merzenich, M.M. (2004). Associative learning shapes the neural code for stimulus magnitude in primary auditory cortex. Proc. Natl. Acad. Sci. USA *101*, 16351–16356.
14. Bao, S., Chang, E.F., Woods, J., and Merzenich, M.M. (2004). Temporal plasticity in the primary auditory cortex induced by operant perceptual learning. Nat. Neurosci. *7*, 974–981.
15. Whitton, J.P., Hancock, K.E., and Polley, D.B. (2014). Immersive audiomotor game play enhances neural and perceptual salience of weak signals in noise. Proc. Natl. Acad. Sci. USA *111*, E2606–E2615.
16. Porter, J., Craven, B., Khan, R.M., Chang, S.J., Kang, I., Judkewitz, B., Volpe, J., Settles, G., and Sobel, N. (2007). Mechanisms of scent-tracking in humans. Nat. Neurosci. *10*, 27–29.
17. Thesen, A., Steen, J.B., and Døving, K.B. (1993). Behaviour of dogs during olfactory tracking. J. Exp. Biol. *180*, 247–251.
18. Polack, P.-O., Friedman, J., and Golshani, P. (2013). Cellular mechanisms of brain state-dependent gain modulation in visual cortex. Nat. Neurosci. *16*, 1331–1339.
19. Bennett, C., Arroyo, S., and Hestrin, S. (2013). Subthreshold mechanisms underlying state-dependent modulation of visual responses. Neuron *80*, 350–357.
20. Fu, Y., Tucciarone, J.M., Espinosa, J.S., Sheng, N., Darcy, D.P., Nicoll, R.A., Huang, Z.J., and Stryker, M.P. (2014). A cortical circuit for gain control by behavioral state. Cell *156*, 1139–1152.
21. Erisken, S., Vaiceliunaite, A., Jurjut, O., Fiorini, M., Katzner, S., and Busse, L. (2014). Effects of locomotion extend throughout the mouse early visual system. Curr. Biol. *24*, 2899–2907.
22. Schneider, K.A., and Kastner, S. (2009). Effects of sustained spatial attention in the human lateral geniculate nucleus and superior colliculus. J. Neurosci. *29*, 1784–1795.
23. Jaramillo, S., Borges, K., and Zador, A.M. (2014). Auditory thalamus and auditory cortex are equally modulated by context during flexible categorization of sounds. J. Neurosci. *34*, 5291–5301.
24. Yang, Y., and Zador, A.M. (2012). Differences in sensitivity to neural timing among cortical areas. J. Neurosci. *32*, 15142–15147.
25. Lee, A.M., Hoy, J.L., Bonci, A., Wilbrecht, L., Stryker, M.P., and Niell, C.M. (2014). Identification of a brainstem circuit regulating visual cortical state in parallel with locomotion. Neuron *83*, 455–466.
26. Wang, X. (2007). Neural coding strategies in auditory cortex. Hear. Res. *229*, 81–93.
27. Letzkus, J.J., Wolff, S.B.E., Meyer, E.M.M., Tovote, P., Courtin, J., Herry, C., and Lüthi, A. (2011). A disinhibitory microcircuit for associative fear learning in the auditory cortex. Nature *480*, 331–335.
28. Jaramillo, S., and Zador, A.M. (2011). The auditory cortex mediates the perceptual effects of acoustic temporal expectation. Nat. Neurosci. *14*, 246–251.
29. Mesgarani, N., and Chang, E.F. (2012). Selective cortical representation of attended speaker in multi-talker speech perception. Nature *485*, 233–236.
30. Steinmetz, N.A., and Moore, T. (2014). Eye movement preparation modulates neuronal responses in area V4 when dissociated from attentional demands. Neuron *83*, 496–506.
31. Lee, A.K.C., Larson, E., Maddox, R.K., and Shinn-Cunningham, B.G. (2014). Using neuroimaging to understand the cortical mechanisms of auditory selective attention. Hear. Res. *307*, 111–120.
32. Bakin, J.S., and Weinberger, N.M. (1996). Induction of a physiological memory in the cerebral cortex by stimulation of the nucleus basalis. Proc. Natl. Acad. Sci. USA *93*, 11219–11224.
33. Bao, S., Chan, V.T., Zhang, L.I., and Merzenich, M.M. (2003). Suppression of cortical representation through backward conditioning. Proc. Natl. Acad. Sci. USA *100*, 1405–1408.
34. Froemke, R.C., Carcea, I., Barker, A.J., Yuan, K., Seybold, B.A., Martins, A.R.O., Zaika, N., Bernstein, H., Wachs, M., Levis, P.A., et al. (2013). Long-term modification of cortical synapses improves sensory perception. Nat. Neurosci. *16*, 79–88.
35. Winkowski, D.E., Bandyopadhyay, S., Shamma, S.A., and Kanold, P.O. (2013). Frontal cortex activation causes rapid plasticity of auditory cortical processing. J. Neurosci. *33*, 18134–18148.
36. Marlin, B.J., Mitre, M., D'amour, J.A., Chao, M.V., and Froemke, R.C. (2015). Oxytocin enables maternal behaviour by balancing cortical inhibition. Nature *520*, 499–504.
37. Crick, F. (1984). Function of the thalamic reticular complex: the searchlight hypothesis. Proc. Natl. Acad. Sci. USA *81*, 4586–4590.
38. Mysore, S.P., and Knudsen, E.I. (2013). A shared inhibitory circuit for both exogenous and endogenous control of stimulus selection. Nat. Neurosci. *16*, 473–478.
39. Bulkin, D.A., and Groh, J.M. (2012). Distribution of eye position information in the monkey inferior colliculus. J. Neurophysiol. *107*, 785–795.
40. Metzger, R.R., Greene, N.T., Porter, K.K., and Groh, J.M. (2006). Effects of reward and behavioral context on neural activity in the primate inferior colliculus. J. Neurosci. *26*, 7468–7476.
41. Edeline, J.M., and Weinberger, N.M. (1991). Subcortical adaptive filtering in the auditory system: associative receptive field plasticity in the dorsal medial geniculate body. Behav. Neurosci. *105*, 154–175.
42. Kastner, S., and Pinsk, M.A. (2004). Visual attention as a multilevel selection process. Cogn. Affect. Behav. Neurosci. *4*, 483–500.
43. Purushothaman, G., Marion, R., Li, K., and Casagrande, V.A. (2012). Gating and control of primary visual cortex by pulvinar. Nat. Neurosci. *15*, 905–912.

Current Biology

Supplemental Information

Locomotion and Task Demands Differentially Modulate Thalamic Audiovisual Processing during Active Search

Ross S. Williamson, Kenneth E. Hancock, Barbara G. Shinn-Cunningham, and Daniel B. Polley

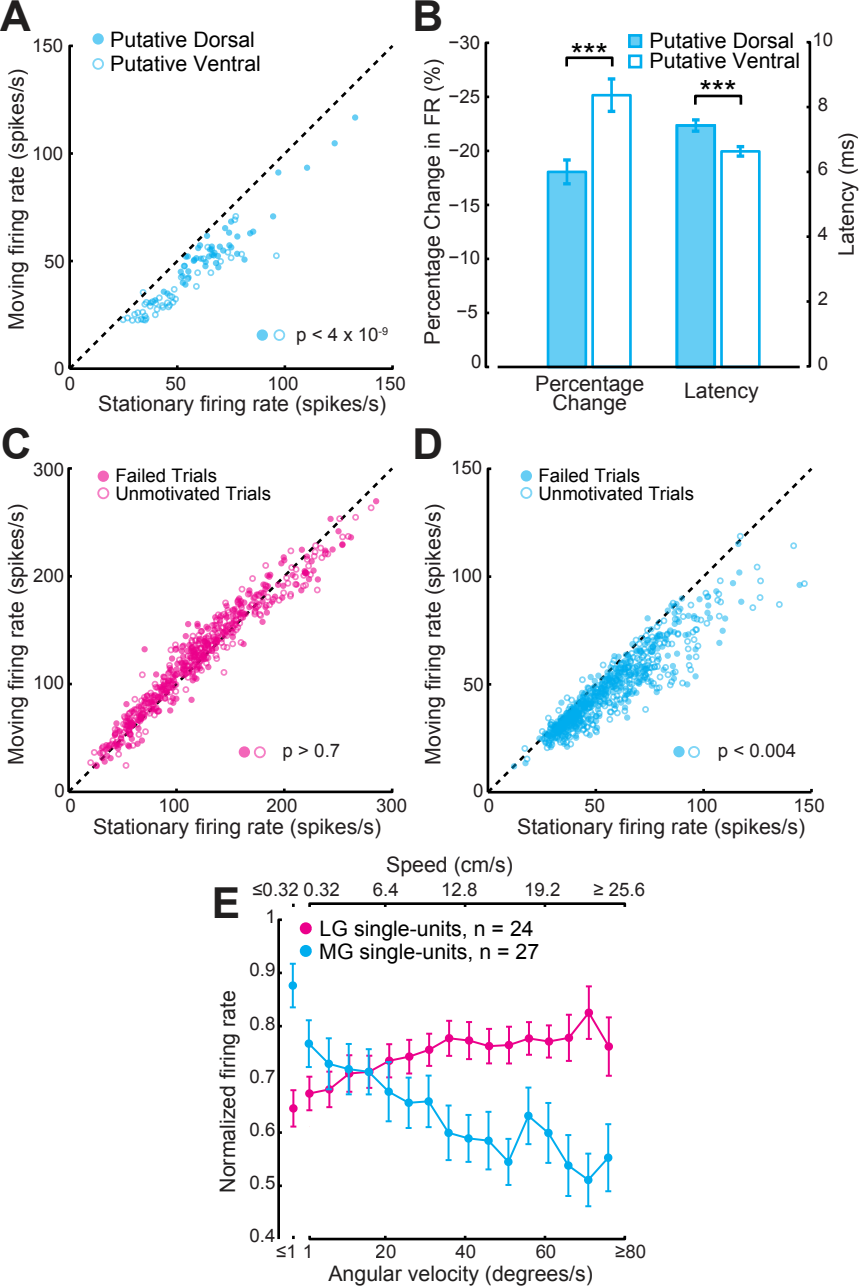
A
Putative Dorsal
Putative Ventral
Moving firing rate (spikes/s)
Stationary firing rate (spikes/s)
p < 4 x 10-9
B
Putative Dorsal
Putative Ventral
***
***
Percentage Change in FR (%)
Latency (ms)
Percentage Change
Latency
C
Failed Trials
Unmotivated Trials
Moving firing rate (spikes/s)
Stationary firing rate (spikes/s)
p > 0.7
D
Failed Trials
Unmotivated Trials
Moving firing rate (spikes/s)
Stationary firing rate (spikes/s)
p < 0.004
E
Speed (cm/s)
≤0.32 0.32 6.4 12.8 19.2 ≥ 25.6
LG single-units, n = 24
MG single-units, n = 27
Normalized firing rate
≤1 1 20 40 60 ≥80
Angular velocity (degrees/s)

Figure S1, Related to Figure 3. Thalamic response modulation remains robust across behavioral states and spatial sampling regions. ***A***, Movement-related suppression is observed for recording sites putatively located in both the dorsal and ventral subdivisions of the MG. Statistical results reflect Wilcoxon Signed-Rank tests. ***B***, Recording sites in the dorsal subdivision have longer sound-evoked response latencies and weaker movement-related suppression than putative ventral recording sites. Values reflect mean ± SEM. Asterisks denote statistically significant differences with a Wilcoxon Rank-Sum test. ***C-D***, Overall movement-related suppression in MG (D), or lack thereof in LG (C), is observed in behavioral trials where mice either failed to identify the TR target region before the trial time expired (filled circles) or ``unmotivated'' trials where the mouse did not rapidly return to the reward spout after tripping the TR target (open circles). Statistical results reflect a bootstrapped ANOVA (as in Fig. 3). ***E***, Modulation of single-unit firing rates in MG and LG across the full range of observed running speeds. Note that the trend closely corresponds to multi-unit data presented in Fig. 3B. Values reflect mean ± SEM.

		Recordings		Mean TR Stimulus Presentations (per session)		Mean TI Stimulus Presentations (per session)		Mean TR Stimulus Presentations (per session)		Mean TI Stimulus Presentations (per session)	
		LG	MG	Stationary	Moving	Stationary	Moving	Off-Target	On-Target	Off-Target	On-Target
Visual = TR	Mouse 1	213	67	981+/-17	3557+/-44	1371+/-23	3860+/-47	4108+/-50	431+/-7	4880+/-61	351+/-5
	Mouse 2	124	21	965+/-89	3537+/-266	1178+/-103	3758+/-281	4096+/-316	406+/-34	4562+/-353	374+/-30
	Mouse 3	30	4	2146+/-90	3412+/-97	2414+/-95	3655+/-102	5237+/-174	321+/-11	5613+/-175	456+/-19
Auditory = TR	Mouse 4	56	0	945+/-37	2218+/-105	1069+/-40	2360+/-109	2990+/-123	172+/-8	3176+/-128	253+/-12
	Mouse 5	0	157	730+/-9	3554+/-36	1053+/-12	3744+/-38	3993+/-41	292+/-3	4466+/-45	332+/-3
	Mouse 6	95	225	893+/-14	4556+/-49	1238+/-17	4845+/-52	5081+/-55	369+/-4	5682+/-62	403+/-4

Table S1, Related to Experimental Procedures. Sample sizes for all conditions.

Supplemental Experimental Procedures

Audiovisual Active Search Task

All procedures performed with mice were approved by the Animal Care and Use Committee at Massachusetts Eye and Ear Infirmary and followed the guidelines established by the National Institutes of Health for the care and use of laboratory animals. All mice were water restricted and their 12h light/dark cycle was reversed. Three mice were chosen to train on the visual search task (with an auditory distractor), and the other three trained on the auditory search task (with a visual distractor).

Mice moved freely within a 10.2 cm wide annular track (track diameter and wall height measured 43.2 cm and 51 cm, respectively) within a sound-attenuating chamber lined with anechoic foam (IAC). Acoustic and visual stimuli were delivered through two high frequency tweeters (Scan Speak; D3004) and four LED's (Visual Instrumentation Corporation, Model 200450) respectively, positioned 55 cm above the floor of the training arena to approximate a homogenous field of illumination and sound intensity. Both auditory and visual stimulus pairs were presented at a rate of 2 Hz (yielding a pair of pulses every 500 ms), with the first flash temporally offset from the first chirp by 0.2 s (***Fig. 1C-D***). Chirps were played at a level of 90 dB SPL, and swept from 100 Hz to 60 kHz, at a rate of 4.29×10^7 Hz/s (which maximally synchronizes activity across auditory nerve fibers by compensating for the inverse relationship between auditory nerve fiber latency and characteristic frequency [S1, S2]. Flashes had a 2 ms strobe width.

The position of the mouse relative to the target was monitored with a webcam (Creative Labs) and custom software (LabVIEW, National Instruments). The inter-pulse interval shifted from 170 to 30 ms or from 200 to 60 ms when the mouse moved into the auditory or visual target regions, respectively. For a single behavioral trial, mice were given 3 minutes to pause within the TR modality target region for a prescribed waiting period (1.5 – 1.75 s), whereupon the behaviorally relevant stimulus terminated and 10 μl of water was made available from a spout in

a fixed location. TR and TI target areas were 28.8˚ wide and were randomly positioned for every trial. We excluded behavioral trials where the mouse was not motivated or not under stimulus control by measuring the time it took to approach the water spout after remaining in the TR region for the required holding time. The water spout approach latencies were fit with a quadratic function in order to account for the distance from the tripped target to the water spout, which caused systematic changes in approach latency. All trials with water spout approach latencies >~3-5 s (dependent on the quadratic threshold) were excluded from behavioral and neurophysiological analysis (but see ***Fig. S1C-D***).

Initially, target areas were large and the required wait times were short to increase the probability of triggering the reward. Wait time and target areas were progressively changed until, at the time of implantation, they were fixed at 1.5 – 1.75 s and 28.8˚, respectively. Choice probabilities were quantified as the percentage of trials in which mice located the target before the time expired. However, when comparing target versus distractor probabilities, a bias was introduced due to the fact that trials ended upon the tripping the target modality but not the distractor target. For this reason, the reported choice probability (***Fig. 2C***) was corrected for analysis purposes by documenting the behavioral choice according to whether the TR or TI target was tripped first.

Behavioral and Neurophysiological Data Analysis

The thalamic recording probe was implanted after approximately 1.5 months of behavioral training (2555 +/- 342 trials). Mice were anesthetized and maintained at a surgical plane of anesthesia with ketamine and xylazine (ketamine: 100 mg/kg, xylazine: 10 mg/kg, maintenance doses were given as required). A homoeothermic blanket system (Fine Science Tools) was used to maintain core body temperature at approximately 36.5˚C. A 2.5 mm wide craniotomy centered 2.75 mm lateral to midline and 2.75 mm caudal to bregma was made atop the right hemisphere under stereotaxic guidance. Silicon oil was applied to the exposed brain surface to prevent drying. A 32-channel silicon probe array (four shanks with eight contacts each, 177 μm^2 contact area, 100 μm inter-contact separation on a single shank, 200 μm inter-

shank separation; Neuronexus) was oriented parallel to the midline and inserted approximately 3 mm deep to access the thalamus. The most caudal shank was positioned to locate the most lateral region that yielded crisp well-driven click responses, which was invariably localized to the ventral subdivision of the MG complex based on prior work [S3, S4] and pilot studies that compared reconstructed lesion sites against post-mortem histology (data not shown). This approach ensured that recordings were made from the dorsal LG on the more rostral shanks.

We identified putative dorsal MG sites (MGd) by locating any vertical penetration with significant sound-evoked responses on 6-8 contact sites on an individual shank in the MG, as the corresponding distance (0.5–0.7 mm) exceeds the dorsal-ventral boundaries of the ventral MG subdivision (MGv) and thus must include at least one recording site in MGd. We excluded recordings from the middle three contacts (as their anatomical location is ambiguous) and labeled the contacts above and below as putative MGd and MGv recordings. Significant movement-related suppression was noted in both putative subdivisions (***Fig. S1A-B***).

In some cases, silicon probes were mounted on a lightweight bi-directional microdrive (HHMI Janelia Farm and Ronal Tool Co), where a lightweight flex cable separated the probe from the connector. In other cases, the silicon probe array was fixed to the connector. Dental cement (C&B Metabond) was used to affix all hardware to the skull. Post-operative analgesia was provided (0.1 mg/kg Buprenex) and a topical antibiotic (Bacitracin) was applied to the wound margin as needed.

Electrophysiological traces were digitized at 32 bit, 24.4 kHz on the headstage (Tucker-Davis Technologies) and stored in binary format. Multi-unit activity was identified adaptively as voltage deflections that exceeded 3.5 SDs from the mean recorded activity (10 s running average). The signals were bandpass filtered at 300-5000 Hz with a fifth-order Butterworth filter. Common average referencing was used to reduce movement related artifacts and improve the quality of the recordings [S5].

Small populations of single-units were identified using OpenSorter (Tucker-Davis Technologies). Sort quality was evaluated using OpenSorter's suite of cluster statistics, and by ensuring that the mode of the ISI histogram was ≥4 ms. All

subsequent analyses were performed in MATLAB (MathWorks) using custom scripts.

Chirp and flash-evoked neural responses were identified on recordings sites where sensory-evoked spiking was at least 3 SD above baseline firing rates. Responses were binned at 5 ms resolution and aligned on the first stimulus within each intra-modality pair to concatenate multiple sensory moments within a single behavioral trial. For each stimulus presentation, the firing rate for each pulse within the pair was computed by averaging activity in a 15 ms window centered on the peak response bin. Spontaneous firing rate was calculated from the 25 ms preceding the first pulse. The mean response to each pulse pair was then matched to the concurrent locomotion status (moving: >1 degree/s, stationary: ≤1 degree/s), the mouse's position within the training arena (inside or outside the TR or TI target regions) and the TR sensory modality. The locomotion criterion of 1 degree/s was chosen for consistency with previous studies [S6-S8]. Given the size of the behavioral arena, this criterion corresponds to between 0.27 and 0.38 cm/s (depending on whether the mouse is running along the inner or outer wall of the track).

PSTH Classifier Model

Population PSTH templates for target and non-target responses were constructed from a subset of the stimulus presentations within a single daily behavioral session. Thalamic ensemble responses to individual stimulus presentations that were not included in the training set were then assigned to the closest population template in Euclidean space. Our response matrix is of dimensionality $RxTN$, where R is the number of stimulus presentations within a given behavioral session (these stimuli s can be either off-target or on-target), T is the number of time bins in the response window (at 1 ms resolution, $T = 500$), and N is the number of units in the ensemble. Because the number of responses in the different conditions varied (off-target versus on-target, and moving versus stationary), classification accuracies were computed using a subsampling

procedure. Fifty subsets of the responses were randomly chosen, such that all behavioral conditions were matched, and population templates could be constructed from the same number of moments from each condition. For each of these subsets, a decoding accuracy was computed as follows.

Classification accuracies were computed using k-fold cross validation, with a 50/50 training/test split. Following [S9], we constructed a dataset matrix of dimensionality $STxNB$. Here, S is the number of stimuli (in this case, $S = 2$), T is the number of trials for each stimulus within a single behavioral session, N is the number of MG or LG units in the ensemble, and B is the number of time bins in the response. Letting $v_{i,j}$ be the i, j^{th}spike count in this matrix, we can define a template for each stimulus s as $\bar{v}^s = [\bar{v}_1^s, \dots, \bar{v}_N^s]$, where the jth element is calculated as

$$\bar{v}_j^s = \frac{1}{T}\sum_{i \epsilon s} v_{i,j}^s$$

and T is the number of trials (in the training set) corresponding to stimulus s. For a single trial in the test set $v_i = [v_{i,1}^s, \dots, v_{i,NB}^s]$ we can then compute the Euclidean distance between each single trial i, and each stimulus template as

$$d_s^i = \sqrt{\sum_{j=1}^{NB}(v_{i,j} - \bar{v}_j^s)^2}$$

A classification is then made according to which stimulus template is closest. Specifically, we obtain a vector of classifications that is the same length as the number of trials in the test set, from which we compute an overall classification accuracy for each fold in the cross-validation. These classification accuracies are then further averaged over the different subsamples to ensure no biasing due to the template matching procedure used.

Statistical Analyses

Significant differences in spontaneous and stimulus-evoked firing rates (***Fig. 3***) were established with a bootstrapped mixed-design ANOVA. Each random bootstrap sample ensured that no unit had more than a 50% chance of being

included in a given draw and that each mouse contributed the same amount of data for each comparison (e.g., moving versus stationary or TR versus TI). The resultant F-values for each ANOVA were compiled into a distribution and evaluated for significance ($p<0.05$) by calculating the proportion of sampled F-values that were greater than the *a-priori* F-value, given the degrees of freedom of the test. Reported F values in the text pertaining to Fig. 3 correspond to the mean F value of the bootstrap distribution. Significant differences in classification accuracies (***Fig. 4***) were established using permutation tests for difference in median (as data were not normally distributed). The Bonferroni correction was used to adjust for multiple comparisons.

Supplemental References

S1. Spankovich, C., Hood, L. J., Wesley Grantham, D., and Polley, D. B. (2008). Application of frequency modulated chirp stimuli for rapid and sensitive ABR measurements in the rat. Hear Res *245*, 92–97.

S2. Taberner, A. M., and Liberman, M. C. (2005). Response properties of single auditory nerve fibers in the mouse. J. Neurophys. *93*, 557–569.

S3. Anderson, L. A., and Linden, J. F. (2011). Physiological differences between histologically defined subdivisions in the mouse auditory thalamus. Hear Res *274*, 48–60.

S4. Hackett, T. A., Barkat, T. R., O'Brien, B. M. J., Hensch, T. K., and Polley, D. B. (2011). Linking topography to tonotopy in the mouse auditory thalamocortical circuit. J Neurosci *31*, 2983–2995.

S5. Ludwig, K. A., Miriani, R. M., Langhals, N. B., Joseph, M. D., Anderson, D. J., and Kipke, D. R. (2009). Using a common average reference to improve cortical neuron recordings from microelectrode arrays. J. Neurophys. *101*, 1679–1689.

S6. Niell, C. M., and Stryker, M. P. (2010). Modulation of visual responses by behavioral state in mouse visual cortex. Neuron *65*, 472–479.

S7. Zhou, M., Liang, F., Xiong, X. R., Li, L., Li, H., Xiao, Z., Tao, H. W., and Zhang, L. I. (2014). Scaling down of balanced excitation and inhibition by active behavioral states in auditory cortex. Nat Neurosci *17*, 841–850.

S8. Erisken, S., Vaiceliunaite, A., Jurjut, O., Fiorini, M., Katzner, S., and Busse, L. (2014). Effects of locomotion extend throughout the mouse early visual system. Curr Biol *24*, 2899–2907.

S9. Foffani, G., and Moxon, K. A. (2004). PSTH-based classification of sensory stimuli using ensembles of single neurons. J Neurosci Methods *135*, 107–120.